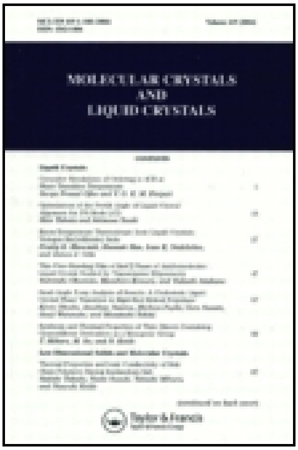

Molecular Crystals and Liquid Crystals Science and Technology. Section A. Molecular Crystals and Liquid Crystals

Publication details, including instructions for authors and subscription information:
http://www.tandfonline.com/loi/gmcl19

Hierarchic Structure of J-Aggregates

Takayoshi Kobayashi [a]

[a] Department of Physics, University of Tokyo, Hongo, Bunkyo, Tokyo, 113, Japan

To cite this article: Takayoshi Kobayashi (1996): Hierarchic Structure of J-Aggregates, Molecular Crystals and Liquid Crystals Science and Technology. Section A. Molecular Crystals and Liquid Crystals, 283:1, 17-24

To link to this article: http://dx.doi.org/10.1080/10587259608037858

Mol. Cryst. Liq. Cryst., 1996, Vol. 283, pp. 17–24
Reprints available directly from the publisher
Photocopying permitted by license only

HIERARCHIC STRUCTURE OF J-AGGREGATES

TAKAYOSHI KOBAYASHI
Department of Physics, University of Tokyo, Hongo, Bunkyo, Tokyo 113, Japan

Abstract We present the dichroic spectra, electroabsorption, wavelength dependence of hole burning efficiency, and intensity dependence of the exciton decay kinetics in the oriented J-aggregates of pseudoisocyanine dye. We propose a new model structure of the J-aggregates. On the low concentration condition the dye molecules form coherent mesoaggregates isotropically distributed. At a high concentration the mesoaggregates start to form incoherently coupled oriented macroaggregates.

INTRODUCTION

J-aggregates of cyanine dyes have attracted many scientists in both fields of physics and chemistry because of their peculiar features, especially J-bands with extremely narrow absorption peak. The structure of J-aggregate has been argued for many years. Recently we developed a new method called "vertical spin coating," with the use of the samples prepared by the method, we found several surprising results, such as large static dipole moment, large wavelength dependence of hole burning efficiency in the J-band. In present paper we shall propose a new model of hierarchic structure of J-aggregates to explain most of the results we obtained.

SAMPLE PREPARATION[1]

Various types of samples were used for the study of the electronic properties of J-aggregates as listed in Table 1. Here in the present paper we used a new method for the preparation of oriented J-aggregates in polymers. 1,1' -diethyl-2,2' -quinocyanine bromide [pseudoisocyanine bromide (PIC-Br)] (Japanese Research Institute for Photosensitizing Dyes, Okayama, Japan) was used without further purification. A few mg of polyvinylalcohol (PVA) with average molecular weight of 300) was dissolved in 2 cm^3 distilled water at ~100°C and during dissolution process the water temperature was heated to ~130°C for PVA to be completely dissolved and 10 mg of PIC-Br was added.

A newly developed "vertical spin coating" (shown in Fig. 1) was used to prepare highly oriented sample films.

TABLE 1 Sample morphologies ever studied and proposed in the present work.

sample	demerit	merit
(1) (aqueous)solution	inconvenient	no inter-aggregate interaction
(2) ethyleneglycol/water-glass	low reproducibility due to cooling rate dependent host-J interaction	narrow spectral width
(3) crystal	large optical density	high symmetry
(4) Langmuir-Blodgett films	disordered, oriented	monolayer
(5) dispersed polymer films	matrix interaction	easy preparation oriented sample

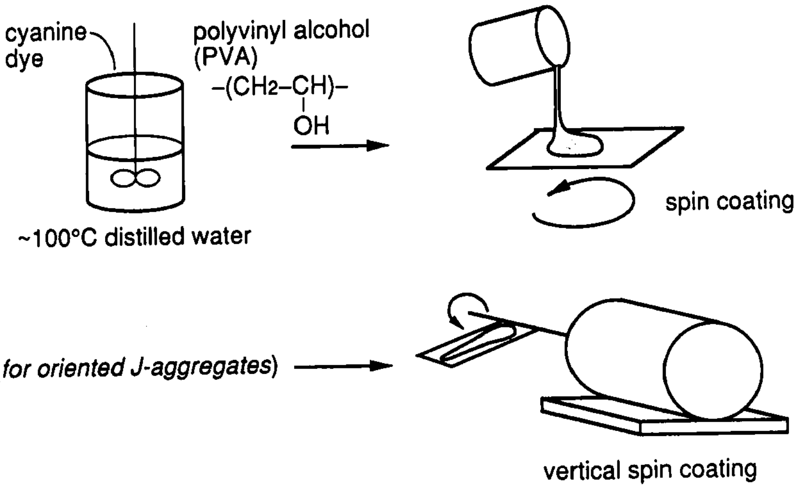

FIGURE 1 Two spin coating methods for the preparation of J aggregates dispersed in polymer films.

DICHROIC SPECTRUM [1-3]

Figure 2 shows the dichroic absorption spectra of samples of several dye concentrations in PVA. A large dichroic ratio, up to 5-10, was observed in the sample PIC - Br/PVA (9 mg/80mg), suggesting the formation of highly oriented J-aggregates. As the PIC concentration was decreased, the dichroic ratio decreased gradually. At weight ratios of 7/80, 6/80 and 4/80, randomly oriented aggregates were obtained simultaneously in the sample films, in addition to well-oriented aggregates along one axis. The randomly oriented aggregates and the oriented ones are presumably different in size; the formers are smaller, while the latters are larger than some critical size needed to be aligned by the fluid dynamical centrifugal force. A remarkable finding is that the J-aggregates become isotropically dispersed around a weight ratio of 3/80. At a ratio lower than 2/80, the J-band disappears and only the monomer spectrum is observed.

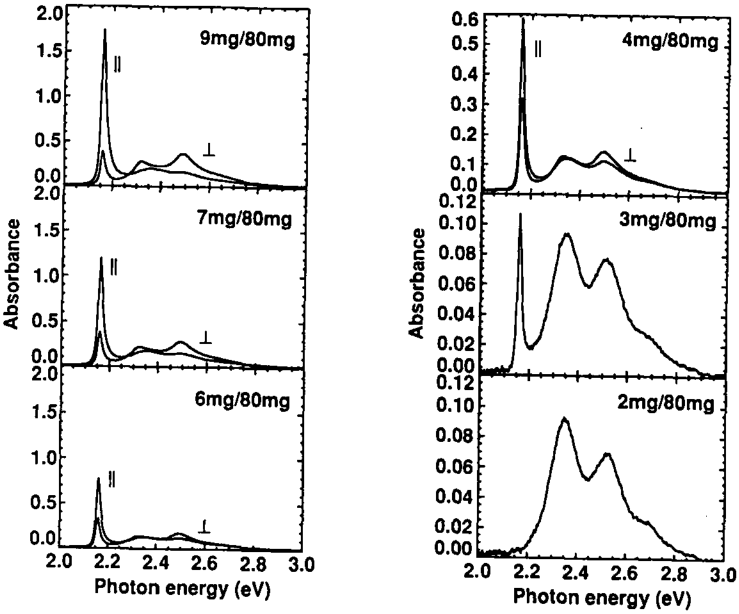

FIGURE 2 The concentration dependence of the dichroic spectra of PIC - Br in IVA. The mixing ratio in weight is from 2mg/80mg to 9mg/80mg.

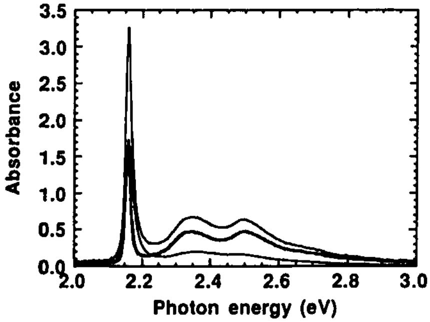

$$A_{\parallel 1} = \sigma_{\parallel}^{\mathrm{or}} N_1^{\mathrm{or}} + \sigma^{\mathrm{coh}} N_1^{\mathrm{coh}}$$
$$A_{\parallel 2} = \sigma_{\parallel}^{\mathrm{or}} N_2^{\mathrm{or}} + \sigma^{\mathrm{coh}} N_2^{\mathrm{coh}}$$

$$A_{\parallel 2} \times \frac{\Delta A_1}{\Delta A_2} - A_{\parallel 1} = \sigma^{\mathrm{coh}} \left(N_2^{\mathrm{coh}} \times \frac{N_1^{\mathrm{or}}}{N_2^{\mathrm{or}}} - N_1^{\mathrm{coh}} \right)$$

FIGURE 3 Spectrum of coherent aggregates (thick curve) calculated from the polarized spectra perpendicular to the orientation at two different concentrations $A_{\parallel i}$ (4mg/80mg for i = 2 and 9mg/80mg for i = 1) and the dichroic spectra $\Delta A_i \equiv A_{\parallel i} - A_{\perp i}$. Top thin curve: $\frac{\Delta A_1}{\Delta A_2} A_{\parallel 2}$. Bottom thin curve $A_{\perp 1}$.

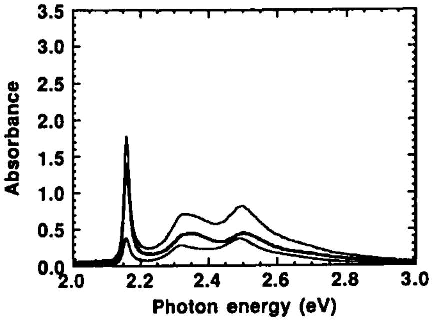

$$A_{\perp 1} = \sigma_{\perp}^{\mathrm{or}} N_1^{\mathrm{or}} + \sigma^{\mathrm{coh}} N_1^{\mathrm{coh}}$$
$$A_{\perp 2} = \sigma_{\perp}^{\mathrm{or}} N_2^{\mathrm{or}} + \sigma^{\mathrm{coh}} N_2^{\mathrm{coh}}$$

$$A_{\perp 2} \times \frac{\Delta A_1}{\Delta A_2} - A_{\perp 1} = \sigma^{\mathrm{coh}} \left(N_2^{\mathrm{coh}} \times \frac{N_1^{\mathrm{or}}}{N_2^{\mathrm{or}}} - N_1^{\mathrm{coh}} \right)$$

FIGURE 4 Spectrum of coherent aggregates (thick curve) calculated from the polarized spectra perpendicular to the orientation at two different concentrations $A_{\perp i}$ (4mg/80mg for i = 2 and 9mg/80mg for i = 1) and the dichroic spectra $\Delta A_i \equiv A_{\parallel i} - A_{\perp i}$. Top thin curve: $\frac{\Delta A_1}{\Delta A_2} A_{\perp 2}$. Bottom thin curve $A_{\perp 1}$.

From the concentration dependence of the absorption spectra of parallel and perpendicular polarizations, the absorption spectra of the J-aggregates are decomposed into those due to isotropically distributed mesoaggregates and oriented macroaggregates as schematically shown in Figs. 3 and 4.

ELECTRIC FIELD EFFECT ON THE ABSORPTION SPECTRUM[4]

The electro-absorption spectra were measured in all the four parallel and perpendicular configurations of both the polarization and static electric field **F** with respect to the oriented axis. The absorbance change due to the Kerr effect is given by,

$$\Delta A_{\text{kerr}} = \frac{1}{2}\frac{\partial^2 A}{\partial E^2}(\Delta\mu\cdot\mathbf{F})^2 - \frac{1}{2}\frac{\partial A}{\partial E}(\mathbf{F}:\Delta\alpha:\mathbf{F}),$$

where $\Delta\mu$, $\Delta\alpha$, A, and E are the static dipole change, the change in the linear polarizability associated with the transition, the linear absorbance, and the photon energy, respectively.

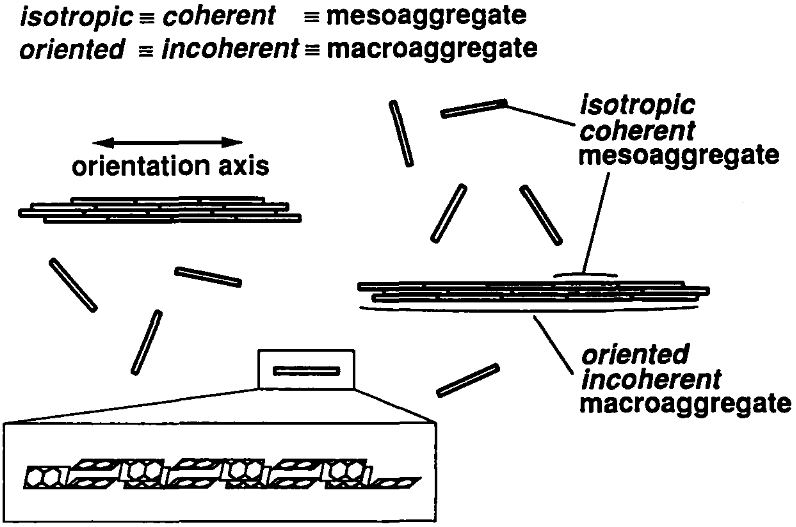

FIGURE 5 Proposed hierarchic structure of J-aggregates.

From all the experimental results we proposed a hierarchic structure of J-aggregates as shown schematically in Fig. 5. By comparing the electroabsorption spectra with the first and second derivatives of the stationary absorption as shown in Fig. 6, it was found that the linear electrooptic spectrum in the region of macroaggregates does not contribute to the first derivatives indicating that the macroaggregates do not have a static dipole moment. This means that the secondary aggregation of mesoaggregates takes place by the static dipole-dipole interaction resulting in the cancellation of the macroscopic static dipole moment in the ground state. Since the formation force of the macroaggregates is not associated with virtual excitation but with the static interaction, the coherence is interrupted among the mesoaggregates, while mesoaggregates are formed by the van de Waals interaction.

The two contributions of $\Delta\mu$ and $\Delta\alpha$ due to mesoaggregates to the absorption change can be decomposed from the electro-absorption spectra in-phase and quadrature-phase to the reference as shown in Fig. 7.

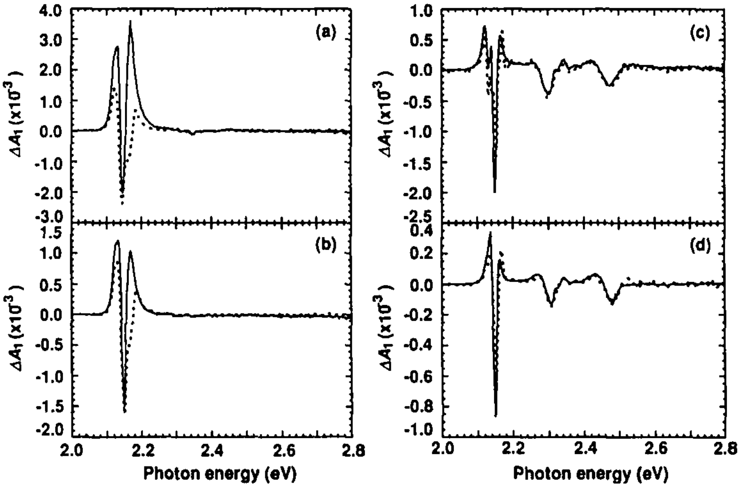

FIGURE 6 Difference absorption spectra due to the Kerr effect. The electric field and the polarization of the light are: both parallel ($F \parallel d$ / $e \parallel d$) (a), perpendicular and parallel ($F \perp d$ / $e \parallel d$) (b), parallel and perpendicular ($F \parallel d$ / $e \perp d$) (c), and both perpendicular ($F \perp d$ / $e \perp d$) (d). The solid and dotted lines are the electro-absorption spectra and the second- and first-derivatives of the linear absorption spectra, respectively.

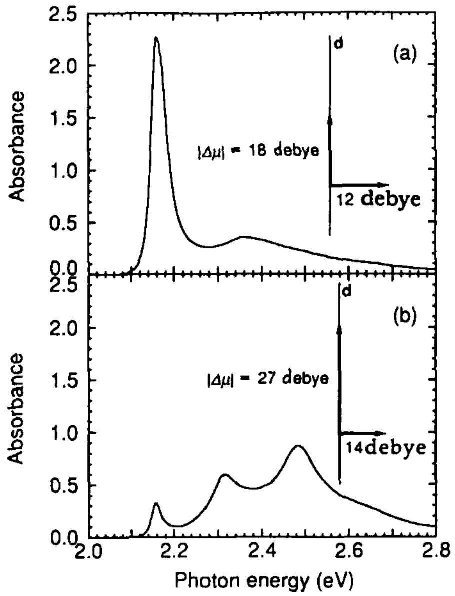

FIGURE 7 Linear absorption spectra for (a) parallel and (b) perpendicular polarization. Inset: change in static dipole moments and polarizability change determined from the electro-absorption spectra.

WAVELENGTH DEPENDENCE OF PHOTOCHEMICAL HOLE-BURNING EFFICIENCY[3,5]

The efficiencies $\eta^{\perp ex}_{\perp pr}$, $\eta^{\perp ex}_{\parallel pr}$, and $\eta^{\parallel ex}_{\perp pr}\cdot A_{\parallel}/A_{\perp}$ obtained from the hole depth in the different polarization configuration are nearly constant around 10^{-4} on the lower energy side of the J-band, and reduce below 10^{-7} on the higher energy side of the band corresponding to the macroscopic incoherent aggregates. This can be explained in terms of $10^{1.5}$ (~ 30) times higher energy transfer rate in the higher energy side of the J-bands. This result implies that the oriented film of J-aggregates contains many isotropic mesoaggregates.

From the value of the $10^{1.5}$ (~ 30) times higher energy transfer rate, the time constant of energy transfer is estimated to be 60ps/30 ≅ 2ps, corresponding to the energy transfer time among mesoaggregates. It takes place from the larger size mesoaggregates with higher energy than that of smaller size mesoaggregates. This energy transfer time is close to the shortened lifetime of the self-quenched exciton life (1 - 2ps) under the high excitation density [6]. In one previous work of femtosecond spectroscopy [6-8], we found that the lifetime of exciton is reduced to 1 - 2ps but it cannot be shorter at even higher exciton densities. This means that the rate determining step of the biexcitonic quenching is the excitonic energy migration among various mesoaggregates and the biexcitonic quenching cannot be faster than this migration process even at the highest exciton density realized in the experiment.

ACKNOWLEDGMENT

The essential contribution of Dr. K. Misawa to the present work is to be acknowledged. The author also thanks Prof. K. Horie, Drs. H. Ono, K. Minoshima, and Mr. S. Machida for their collaboration.

The work was partly supported by a Grant-in-Aid for Specially Promoted Research from the ministry of Education, Science, and Culture NO. 051020021.

REFERENCES

1. K. Misawa, H. Ono, K. Minoshima, and T. Kobayashi, Appl. Phys. Lett. 63, 577 (1978).
2. K. Misawa, H. Ono, K. Minoshima, and T. Kobayashi, J. Lumin., 60&61, 817 (1994).
3. K. Misawa, S. Machida, K. Horie, and T. Kobayashi, Chem. Phys. Lett. 240, 210 (1994).
4. K. Misawa, K. Minoshima, H. Ono, and T. Kobayashi, Chem. Phys. Lett. 220, 251 (1994)
5. K. Misawa, S. Machida, K. Horie, and T. Kobayashi, J. Lumin., 64, 239 (1994).
6. K. Minoshima, M. Taiji, K. Misawa, and T. Kobayashi, Chem. Phys. Lett. 218, 67 (1994).
7. K. Misawa, K. Minoshima, and T. Kobayashi, Chem. Phys. Lett. 220, 251 (1994).
8. K. Minoshima, M. Taiji, A. Ueki, K. Miyano, and T. Kobayashi, Proceedings of 4th International Conference of Optically Nonlinear Organic Materials and Applications, Hawaii Island, USA, 17-20 May, 1994.